

Early–Late Heterobimetallic Alkoxides as Model Systems for Late-Transition-Metal Catalysts Supported on Titania

Rosa Fandos,^[a] Carolina Hernández,^[a] Antonio Otero,^{*,[b]} Ana Rodríguez,^[c] María José Ruiz,^[a] and Pilar Terreros^[d]

Abstract: Titanium complexes with chelating alkoxide ligands [TiCp*(O₂Bz)(OBzOH)] (**1**) and [TiCp*(Me){(OCH₂)₂Py}] (**2**) were synthesised by reaction of [TiCp*Me₃] (Cp* = η⁵-C₅Me₅) with 2-hydroxybenzyl alcohol ((HO)₂Bz) and 2,6-pyridinedimethanol ((HOCH₂)₂Py), respectively. Complex **1** reacts with [[M(μ-OH)(cod)]₂] (M = Rh,

Ir) to yield the early–late heterobimetallic complexes [TiCp*(O₂Bz)₂M(cod)] [M = Rh (**3**), Ir (**4**)]. Carbon monoxide readily replaces the COD ligand in **3** to

Keywords: heterometallic complexes • iridium • O ligands • rhodium • titanium

give the rhodium dicarbonyl derivative [TiCp*(O₂Bz)₂Rh(CO)₂] (**5**). Compound **2** reacts with [[M(μ-OH)(cod)]₂] (M = Rh, Ir) with protonolysis of a Ti–Me bond to give [TiCp*{(OCH₂)₂Py}(μ-O)M(cod)] [M = Rh (**6**), Ir (**7**)]. The molecular structures of complexes **3**, **5** and **7** were established by single-crystal X-ray diffraction studies.

Introduction

The synthesis and study of the reactivity of transition-metal alkoxides and aryloxides continues to be an area of research interest on account of their relevance to areas such as biology^[1] and catalysis. In catalysis they have been used as precursors for homogeneous α-olefin polymerisation catalysts,^[2] for enantioselective carbon–carbon bond-forming reactions^[3] and as models for heterogeneous systems. In particular, early-transition-metal alkoxides can be envisaged as models of heterogeneous catalyst supports,^[4] and early–late heterometallic complexes can be used as models to

provide insight into the chemistry at the interface between a metal and its oxide support.^[5] In catalysis modulation of the nature of the active sites is very important. In this regard, the geometry of Ti centres in mixed oxides has been broadly studied in order to correlate it with the catalytic performance. Another important phenomenon is the strong metal support interaction (SMSI) observed when late transition metals on reducible oxides are reduced in hydrogen at high temperature (773 K), which induces dramatic changes in product selectivity.^[6] Furthermore, immobilisation of organometallic compounds on solid surfaces such as oxides, zeolites and metals is a field of growing interest^[7] on account of the highly active surface species involved in heterogeneous catalysis. However, as in the case of the classical heterogeneous catalysts, the nature of the bonding and the mechanism by which the metal precursor reacts is not fully understood. Therefore, obtaining three-dimensional molecular model compounds is of interest for more exactly identifying the species present on the surface of a support and understanding the bonding between metals and oxide surfaces and how these properties are related to the catalytic activity.^[8]

Here we report the synthesis of two new dialkoxide titanium complexes [TiCp*(O₂Bz)(OBzOH)] (**1**) and [TiCp*(Me){(OCH₂)₂Py}] (**2**), which can be regarded as models for the above-mentioned systems. Moreover, we studied the reactions of **1** and **2** with [[M(μ-OH)(cod)]₂] (M = Rh, Ir), which give the corresponding early–late heterometallic complexes. These compounds can be considered as molecular models for late-transition-metal catalysts supported on titania.

[a] Dr. R. Fandos, Dr. C. Hernández, Dr. M. J. Ruiz
Departamento de Química Inorgánica, Orgánica y Bioquímica
Universidad de Castilla-La Mancha
Facultad de Ciencias del Medio Ambiente
Avd. Carlos III, s/n, 45071 Toledo (Spain)

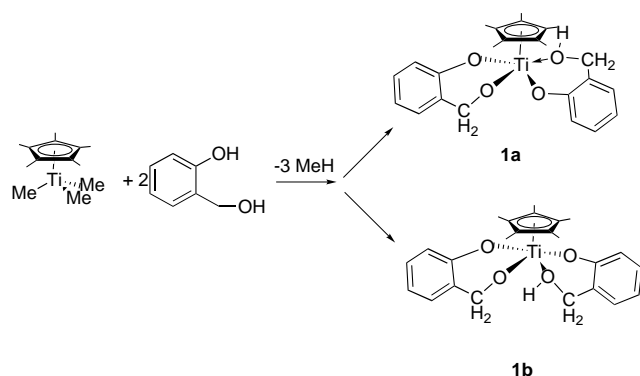
[b] Prof. Dr. A. Otero
Departamento de Química Inorgánica, Orgánica y Bioquímica
Universidad de Castilla-La Mancha, Facultad de Químicas
Campus de Ciudad Real, Avd. Camilo José Cela, 10
13071 Ciudad Real (Spain)

[c] Dr. A. Rodríguez
Departamento de Química Inorgánica, Orgánica y Bioquímica
Universidad de Castilla-La Mancha
ETS Ingenieros Industriales, Campus de Ciudad Real
Avd. Camilo José Cela, 3
13071 Ciudad Real (Spain)

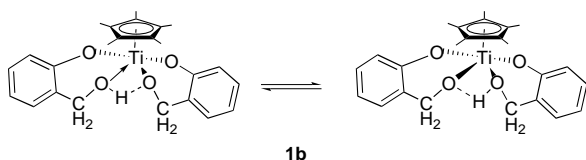
[d] Dr. P. Terreros
Instituto de Catálisis y Petroleoquímica, CSIC
Cantoblanco, 28049 Madrid, (Spain)

Results and Discussion

The titanium complex $[\text{TiCp}^*(\text{Me})_3]$ reacts with 2-hydroxybenzyl alcohol to yield **1** (Scheme 1), which was isolated as a mixture of two isomers in good yield (73%). It is soluble in most common organic solvents. Complex **1** was characterized by NMR spectroscopy. In accordance with its ^1H and ^{13}C NMR spectra, we propose complex **1** to be a monomer in which two alkoxide ligands are bonded to the titanium centre in a bidentate fashion. Thus, the remaining hydroxyl group can coordinate through a dative bond to the metal centre *trans* (**1a**) or *cis* (**1b**) to the benzyloxy moiety (see Scheme 1).

Scheme 1. Synthesis of **1**.

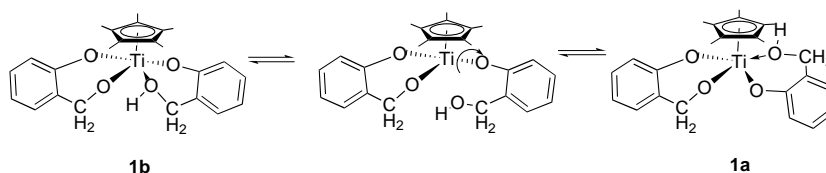
The ^1H NMR spectrum is in agreement with this proposal. It shows two singlets at $\delta = 1.69$ and 1.78 , which are assigned to the Cp^* ligand of each isomer, three AB spin systems for the methylene groups, and several multiplets corresponding to the aromatic protons. The hydroxylic protons appear as two broad signals at $\delta = 4.23$ and 7.26 ppm. The $^{13}\text{C}\{^1\text{H}\}$ NMR spectrum confirms the presence of three different environments for the methylene carbon atoms and shows three signals at $\delta = 72.0$, 72.1 and 75.3 ppm. These data indicate a rapid proton transfer in **1b** that would make the two methylene groups of the molecule equivalent (see Scheme 2).

Scheme 2. Proton transfer in **1b**.

The proton exchange is rapid on the NMR timescale, even at 193 K. Hydrogen bonding in these systems is an important feature, since hydrolysis and condensation reactions are often carried out in the presence of alcohol solvents.^[9]

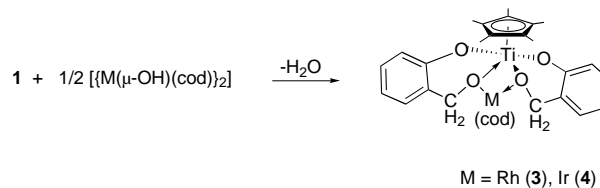
Furthermore, a variable-temperature NMR experiment showed that the ratio of **1a** and **1b** does not change between

193 and 338 K. Above this temperature, the ^1H NMR signals become broader, and at 353 K the methylene signals coalesce. At 371 K, the spectrum shows a singlet at $\delta = 1.92$ ppm for the Cp^* ligand and two broad signals at $\delta = 5.03$ and 5.44 ppm for the OH and the methylene protons, respectively. These data, although the rapid-exchange limit spectrum was not reached in this temperature range, indicate the rapid interchange proposed in Scheme 3, by which both isomers **1a** and **1b** and

Scheme 3. Proposed high-temperature interchange in **1**.

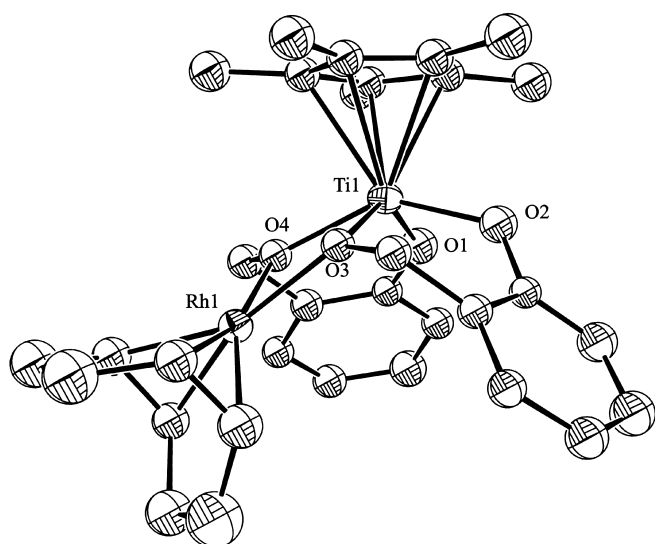
the two dialkoxide ligands would become equivalent on the NMR timescale.

Complex **1** reacts with $[\{\text{M}(\mu\text{-OH})(\text{cod})\}_2]$ ($\text{M} = \text{Rh}, \text{Ir}$) to yield, through a condensation reaction, the heterobimetallic complexes $[\text{TiCp}^*(\text{O}_2\text{Bz})_2\text{M}(\text{cod})]$ ($\text{M} = \text{Rh}$ (**3**), Ir (**4**); Scheme 4). Complexes **3** and **4** are rather air-stable in the solid state, slightly soluble in alkanes, and very soluble in

Scheme 4. Synthesis of **3** and **4**.

toluene and THF. They were characterized by ^1H and ^{13}C NMR spectroscopy. The ^1H and ^{13}C NMR spectra are consistent with a symmetric coordination environment of the metal centres. For example, the ^1H NMR spectrum of complex **4** shows two multiplets at $\delta = 3.52$ and 3.63 ppm (both 2H) for the two sets of olefinic protons in the COD ligand. In addition, multiplets at $\delta = 0.97$, 1.32 , 1.49 and 2.10 ppm (total 8H) correspond to the methylene protons of the cyclooctadiene ligand. The methylene protons of the two equivalent alkoxide groups give two doublets at $\delta = 4.02$ and 4.84 ppm.

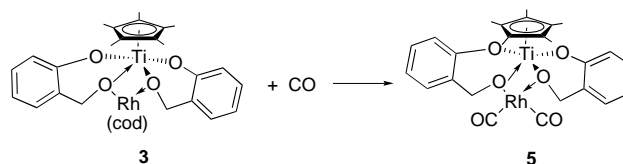
To confirm the proposed structure, orange crystals of **3** suitable for X-ray diffraction were obtained by slow diffusion of pentane into a saturated solution of **3** in toluene. Figure 1 shows an ORTEP plot, and selected geometrical parameters are listed in Table 1. The structure is built up of discrete bimetallic (TiRh) molecules. The geometry around the titanium atom is square-pyramidal, and that around the rhodium atom roughly planar. The midpoints of the two $\text{C}=\text{C}$ (COD) bonds, the two oxygen atoms bound to rhodium and the rhodium atom are coplanar to within 0.093 \AA . The distance from the titanium atom to the plane containing the cyclopentadienyl ring ($2.065(2) \text{ \AA}$) is normal for titanium complexes.^[10] The Ti1-O1 and Ti1-O2 distances of $1.877(6)$ and $1.888(6) \text{ \AA}$, respectively, are somewhat longer than those

Figure 1. ORTEP plot of **3** with 30% thermal ellipsoids.

in other titanium complexes with aryloxy ligands.^[11] On the other hand, the Ti1–O3 and Ti1–O4 distances are longer (2.029(6) and 2.026(6) Å, respectively), as expected for bridging alkoxide ligands.^[12] The Ti1–O3–Rh1 and Ti1–O4–Rh1 angles are 105.4(2) and 106.3(3)°, respectively. The Rh–Ti distance of 3.255(2) Å is long enough to rule out a direct metal–metal interaction.^[5] For comparison, the Ti–Rh distance in an alloy of the metals is 2.68 Å, while in a highly reduced Rh on titania, the Ti–Rh bond length is 2.55 Å.^[13]

Heterometallic complex **3** reacts with an excess of carbon monoxide at room temperature under atmospheric pressure

with displacement of COD to yield the dicarbonyl complex **5** (Scheme 5). Complex **5** was isolated in 73% yield as air-stable orange crystals and was spectroscopically characterized. The

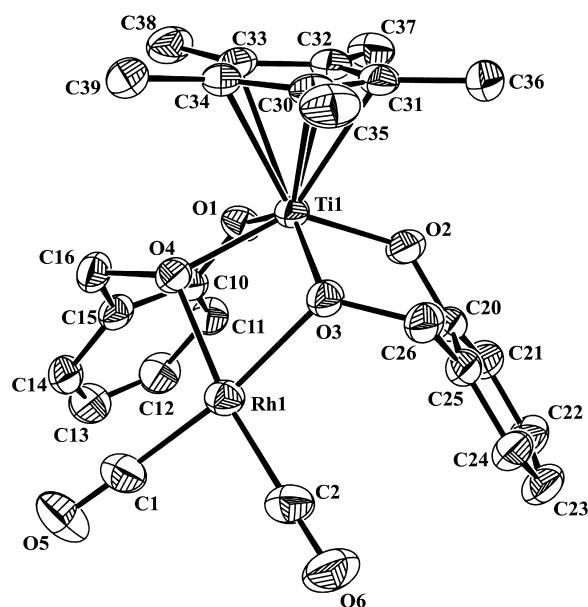
Scheme 5. Synthesis of **5**.

pattern and the relative intensity of the $\nu(\text{CO})$ bands at 2066 and 1997 cm^{-1} in the IR spectrum is as expected for a *cis*-dicarbonylrhodium(i) complex.^[14] These can be envisaged as the ν_{sym} and ν_{asym} of geminal $\text{Rh}^+(\text{CO})_2$ species in surface Rh/TiO₂ catalysts.^[15] The ¹H and ¹³C NMR spectra are also consistent with the proposed structure. The ¹H NMR spectrum exhibits two doublets for the methylene groups of the two equivalent alkoxide ligands, while in the ¹³C NMR spectrum the signal corresponding to the two equivalent carbonyl ligands appears at $\delta = 183.4$ ppm.

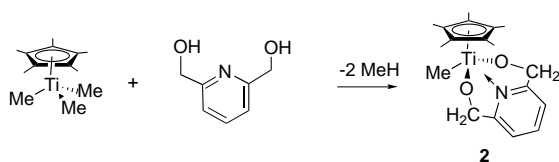
The molecular structure of complex **5** was confirmed by X-ray crystallography. The ORTEP plot of the molecule and the atom-labelling scheme are shown in Figure 2, and Table 1 lists selected bond lengths and angles. The structure is similar to that of **3**. The geometry around the titanium atom is square-pyramidal, and that around the rhodium atom approximately planar. The Ti–O bond lengths are within the range expected for this type of compounds, but somewhat longer than in complex **3**. The Rh1–Ti1 bond length of 3.1383(9) Å is shorter than that of **3**.

Table 1. Selected bond lengths [Å] and angles [°] for **3**, **5** and **7**.

	3	5	7
Rh1–O4	2.041(5)	Rh1–C2	1.855(6)
Rh1–O3	2.063(5)	Rh1–C1	1.866(6)
Rh1–C45	2.088(10)	Rh1–O4	2.029(3)
Rh1–C41	2.100(10)	Rh1–O3	2.035(3)
Rh1–C40	2.101(10)	Ti1–O1	1.900(3)
Rh1–C44	2.105(10)	Ti1–O2	1.908(3)
Ti1–O1	1.877(6)	Ti1–O4	2.046(3)
Ti1–O2	1.888(6)	Ti1–O3	2.049(3)
Ti1–O4	2.026(6)		
Ti1–O3	2.029(6)		
O4–Rh1–O3	72.5(2)	C2–Rh1–C1	88.5(2)
O1–Ti1–O2	89.1(3)	O4–Rh1–O3	72.1(1)
O1–Ti1–O4	84.3(2)	O1–Ti1–O2	91.5(1)
O2–Ti1–O4	140.5(3)	O1–Ti1–O4	83.8(1)
O1–Ti1–O3	135.1(3)	O2–Ti1–O4	136.8(1)
O2–Ti1–O3	84.5(3)	O1–Ti1–O3	136.7(1)
O4–Ti1–O3	73.5(2)	O2–Ti1–O3	83.9(13)
C15–O1–Ti1	136.8(6)	O4–Ti1–O3	71.4(1)
C25–O2–Ti1	128.8(6)	C10–O1–Ti1	130.5(3)
C2–O3–Ti1	122.6(5)	C20–O2–Ti1	129.9(3)
C2–O3–Rh1	126.1(5)	C26–O3–Rh1	121.6(3)
Ti1–O3–Rh1	105.4(2)	C26–O3–Ti1	121.0(3)
C1–O4–Ti1	122.7(5)	Rh1–O3–Ti1	100.4(1)
C1–O4–Rh1	128.5(5)	C16–O4–Rh1	121.1(3)
Ti1–O4–Rh1	106.3(3)	C16–O4–Ti1	121.2(3)
		Rh1–O4–Ti1	100.7(1)
		O2–Ir1–O2	2.05(3)
		Ir1–O1	2.03(2)
		Ir1–C12	2.05(4)
		Ir1–C9	2.03(4)
		Ir1–C13	2.07(4)
		Ir1–C8	2.12(4)
		Ti1–O1	1.73(3)
		Ti1–O3	1.89(3)
		Ti1–O2	2.09(3)
		Ti1–N1	2.18(3)
		O2–Ir1–O1	77.1(10)
		O1–Ti1–O3	99.1(13)
		O1–Ti1–O2	83.1(12)
		O3–Ti1–O2	139.0(11)
		Ti1–O1–Ir1	106.1(11)
		C1–O2–Ir1	129(3)
		C1–O2–Ti1	123(3)
		Ir1–O2–Ti1	93.4(11)
		C7–O3–Ti1	128(3)

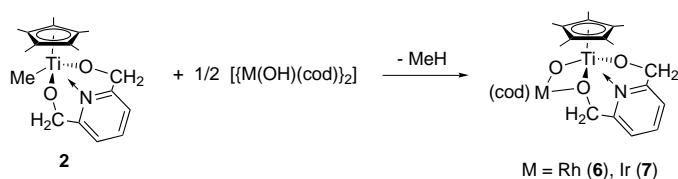
Figure 2. ORTEP plot of **5** with 30% thermal ellipsoids.

The titanium complex $[\text{TiCp}^*(\text{Me})_3]$ reacts with 2,6-pyridinedimethanol to yield **2** (Scheme 6), which was isolated in good yield (78%) as a bright yellow air-sensitive solid. It is

Scheme 6. Synthesis of **2**.

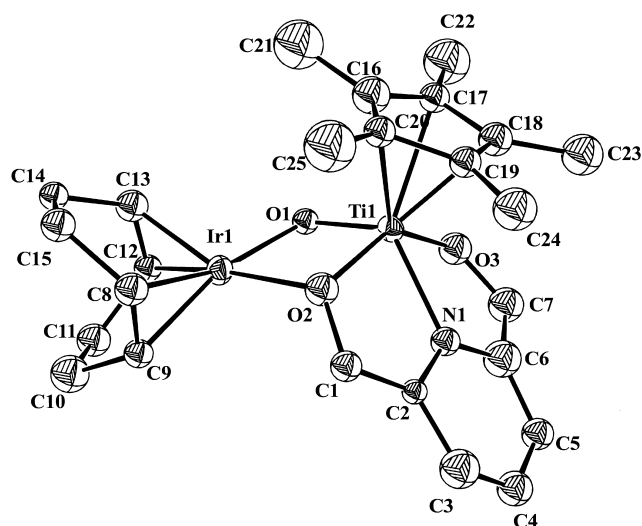
rather soluble in THF and toluene, and less soluble in pentane. It was spectroscopically characterized. The ^1H NMR spectrum shows a singlet at $\delta = 0.12$ ppm for the methyl group bonded to the titanium centre and a signal for the Cp* ligand at $\delta = 2.11$ ppm. Two doublets at $\delta = 5.49$ and 5.60 ppm correspond to the two equivalent methylene groups of the dialkoxide ligand. Hence, we propose complex **2** to be a monomer in which two oxygen atoms of the dialkoxide ligand and the pyridine nitrogen atom are bonded to the titanium centre in a symmetrical coordination environment of the metal centre.

Complex **2** undergoes a protonolysis reaction with $[\{\text{M}(\mu\text{-OH})(\text{cod})\}_2]$ ($\text{M} = \text{Rh}, \text{Ir}$) to yield the heterobimetallic complexes $[\text{TiCp}^*\{(\text{OCH}_2)_2\text{Py}\}(\mu\text{-O})\text{M}(\text{cod})]$ ($\text{M} = \text{Rh}$ (**6**), Ir (**7**); Scheme 7), which were isolated as yellow solids, sparingly soluble in pentane, toluene and THF, and more soluble in

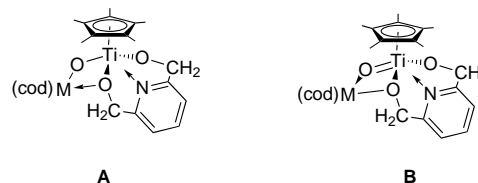
Scheme 7. Synthesis of **6** and **7**.

chloroform. They were characterized spectroscopically. The ^1H and ^{13}C NMR spectroscopic data indicate similar structures for **6** and **7**. The ^1H NMR spectra show that the methylene groups of the alkoxide ligand are in different chemical environments, as is expected if one of the oxygen atoms of the dialkoxide moiety is bonded both to the late-transition-metal centre and to the titanium atom, and the other only to the titanium centre. Furthermore, in agreement with this proposal, all four olefinic protons of the COD ligand are different. The ^{13}C NMR spectrum confirms the different chemical environments of the methylene groups.

A single-crystal X-ray diffraction study on **7** confirmed the predicted structure. Figure 3 shows an ORTEP plot and the atom-labelling scheme of **7**, and selected bond lengths and angles are listed in Table 1. As expected, the asymmetric unit contains both enantiomers. The molecule consists of discrete bimetallic units in which the titanium and iridium atoms are bridged by two oxygen atoms, one from the alkoxide ligand and an oxo group. The geometry around the iridium centre is approximately square-planar, and that around the titanium atom square-based pyramidal. The Ti1-O1 distance of $1.73(3)$ Å is at the short end of the range expected for $\mu\text{-oxo}$

Figure 3. ORTEP plot of **7** with 30% thermal ellipsoids.

titanium compounds.^[16] On the other hand, Ti1-O2 is rather long ($2.09(3)$ Å), but within the expected range for bridging alkoxide ligands.^[12] In contrast to the highly unsymmetrical Ti–O distances, the Ir1-O1 and Ir1-O2 bond lengths are quite similar ($2.03(2)$ and $2.05(3)$ Å, respectively). These structural parameters may indicate a certain contribution of form **B** (see Scheme 8) to the bonding of the four-membered ring in **7**. Unfortunately, no other complexes in which Ti and Ir are bridged by oxygen atoms have been structurally characterized. Alternatively, the Ti–Ir bond length ($3.012(7)$ Å) might indicate an Ir–Ti dative bonding interaction.^[17]

Scheme 8. Bonding modes for **6** and **7**.

X-ray photoelectron spectroscopy (XPS) was used to compare the binding energies (BE) of **1**, **3**, **4**, **5** and **6** with those of some heterogeneous catalysts and to give information on the steric and electronic influence of the ligands on the metal atom. The binding energies of the core electrons are listed in Table 2. Knowledge of the coordination environment of Ti^{4+} in oxides and the electron density is very important for modulating the catalytic performance of solid catalysts. The geometry around the titanium atom in the compounds

Table 2. XPS binding energies [eV] of core electrons of compounds **1**, **3**, **4**, **5** and **6**.

Compound	C 1s	O 1s	Ti 2p _{3/2}	Rh 3d _{5/2}	Ir 4f _{7/2}	N 1s
1	284.6	531.2	457.6			
3	284.5	531.1	457.4	308.6		
5	284.6	531.2, 534.0	457.5	309.1		
6	284.5	530.4	457.3	308.2		399.3
4	284.5	531.5	457.5		61.6	

reported here is square-pyramidal, and the formal oxidation state is +4. The Ti 2p_{3/2} BE (457.6 eV) of **1** is slightly higher than those of the heterobimetallic Ti–Rh (**3**, **5** and **6**) and Ti–Ir (**4**) complexes (457.4, 457.5, 457.3 and 457.5 eV, respectively; Figure 4). These values are somewhat lower than those reported for Ti⁴⁺ in titania^[18] (458.4 or 458.5 eV), in a titanium-substituted SSZ42 zeolite^[19a] in tetrahedral and octahedral sites (459.8 and 458.3 eV, respectively) and in SiO₂-supported titanium (460.0 (*T_d*), 458.5 (*O_h*)).^[19b] This is probably due to the electronic effect of the Cp* ligand.^[20] On reduction to Ti³⁺ the BE shifts to about 454.6 eV.

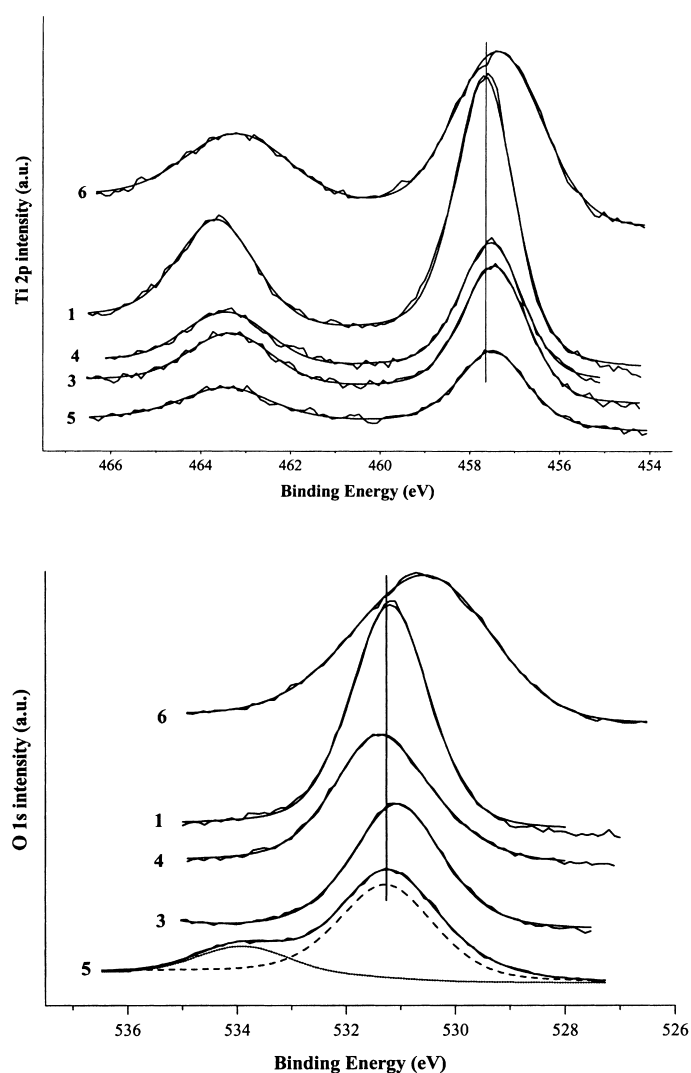


Figure 4. XPS spectra. Ti (2p) and O (1s) regions of **1**, **3**, **4**, **5** and **6**.

In compounds **3**, **5** and **6** the Rh 3d_{5/2} BE (308.6, 309.1 and 308.2 eV, respectively) is in agreement with oxidation state +1.^[21] The increase of 0.5 eV between **3** and **5**, in which COD has been substituted by CO, is probably due to depletion of charge on the rhodium atom by π back-donation in the Rh–CO bond. This is in accordance with the situation in monodispersed *gem*-Rh⁺(CO)₂ species on oxide supports, a very important phase of supported Rh on oxide catalysts.^[22] The core level C1s binding energies are practically the same for all compounds. The ligand effect on O1s binding energies

is more evident. Compounds **1**, **3**, **4** and **5**, derived from 2-hydroxybenzyl alcohol, show a peak centred at 531.1–531.5 eV, while for **6**, derived from 2,6-pyridinedimethanol, this peak appears at 530.4 eV. The last named complex has a different coordination environment, and the presence of the N donor should affect the electronic density on the O atoms. The peak 534.0 eV for **5** (Figure 4) can be assigned to the carbonyl groups.

Thus the Ti⁴⁺ 2p_{3/2} BE is not very sensitive to changes in the coordination mode or the presence of a Ti–O–M (M = Rh, Ir) moiety, whereas the Rh⁺ 3d_{5/2} BE reflects the nature of the ligand in the Ti sphere, especially when a *gem*-Rh(CO)₂ moiety is formed by substitution of COD. The oxygen 1s BE of the Ti–O–M bond also reflects these differences and is separated from the carbonyl oxygen BE by 3 eV; it could be important in studying the interaction of the Rh carbonyl species with the reactants in the catalytic process.

In conclusion, we have synthesised two new dialkoxide titanium complexes, which were used for the preparation of four early–late heterometallic complexes which can be regarded as molecular models of rhodium and iridium catalysts supported on titania.

Experimental Section

General procedures: All compounds were prepared and handled with rigorous exclusion of air and moisture under nitrogen atmosphere by using standard vacuum line and Schlenk techniques. All solvents were dried and distilled under nitrogen.

The following reagents were prepared by literature procedures: [TiCp*(Me)₃]₃,^[23] [[Rh(μ -OH)(cod)]₂]₂,^[24] [[Ir(μ -OH)(cod)]₂]₂.^[25] The commercially available compounds (HO)₂Bz, (HOCH₂)₂Py and LiMe in diethyl ether were used as received from Aldrich.

¹H and ¹³C NMR spectra were recorded on 200 Mercury Varian Fourier Transform spectrometer. Trace amounts of protonated solvents were used as references, and chemical shifts are reported in parts per million relative to SiMe₄. IR spectra were recorded in the range 4000–400 cm⁻¹ with a Nicolet Magna-IR 550 spectrophotometer.

Photoelectron spectra (XPS) were acquired with a VG Escalab 200R spectrometer fitted with a MgK α ($h\nu = 1253.6$ eV) 120 W X-ray source and a hemispherical electron analyser. A DEC PDP 11/53 computer was used for collecting and processing the spectra. The powder samples were pressed into small Inox cylinders, mounted on a sample rod, placed in a pretreatment chamber and outgassed at 298 K and 10⁻⁵ Torr for 5 h prior to being transferred to the analysis chamber. The residual pressure during data acquisition was maintained below 3 \times 10⁻⁹ Torr. Accurate binding energies (± 0.2 eV) were determined by referencing to the C 1s peak at 284.6 eV.

[TiCp*(O₂Bz)(OBzOH)] (1): (HO)₂Bz (0.217 g, 1.76 mmol) was added to a solution of [TiCp*(Me)₃] (0.200 g, 0.88 mmol) in toluene (5 mL) at –40 °C. The mixture was allowed to warm to room temperature and was stirred for 1 h. After filtration, the solvent was removed under vacuum and the residue washed with pentane (5 mL) to yield **1** as a red solid. Yield: 0.275 g, 73 %; IR: $\tilde{\nu} = 3437$ (br), 1594 (m), 1573 (m), 1480 (s), 1448 (s), 1265 (vs), 1109 (w), 1009 (m), 885 (m), 752 (s), 634 (m), 498 cm⁻¹ (m); ¹H NMR ([D₆]benzene, RT, 200 MHz): $\delta = 1.69$ (s, Cp*), 1.78 (s, Cp*), 4.23 (br, OH), 5.03 (d, $J = 16.13$ Hz, OCH₂), 5.09 (d, $J = 13.56$ Hz, OCH₂), 5.22 (d, $J = 16.86$ Hz, OCH₂), 5.32 (d, $J = 16.86$ Hz, OCH₂), 5.40 (d, $J = 16.13$ Hz, OCH₂), 5.70 (d, $J = 13.56$ Hz, OCH₂), 6.68–7.20 (m, Ar), 7.26 ppm (br, OH); ¹³C NMR [¹H]: 12.2 (s, Cp*), 12.3 (s, Cp*), 72.0 (s, OCH₂), 72.1 (s, OCH₂), 75.3 (s, OCH₂), 117.6 (s, Ar), 118.3 (s, Ar), 118.7 (s, Ar), 125.4 (s, Ar), 125.9 (s, Ar), 126.0 (s, Ar), 126.2 (s, Cp*), 126.9 (s, Cp*), 128.1 (s, Ar), 128.2 (s, Ar), 128.4 (s, Ar), 128.5 (s, Ar), 128.6 (s, Ar), 128.9 (s, Ar), 163.0 (s, *ipso*), 163.8 (s, *ipso*), 163.9 ppm (s, *ipso*); elemental analysis calcd (%) for C₂₄H₂₈O₄Ti: C 67.29, H 6.58; found: C 67.88, H 6.62.

[TiCp*(O₂Bz)₂Rh(cod)] (3): Toluene (6 mL) was added to a mixture of **1** (0.200 g, 0.47 mmol) and [[Rh(μ -OH)(cod)]₂] (0.107 g, 0.47 mmol) at room temperature. The mixture was stirred for 2 h and then the solvent was partially evaporated under vacuum. Slow diffusion of pentane into the toluene solution yielded orange crystals of **3**. Yield: 0.158 g, 53%; IR: $\tilde{\nu}$ = 1595 (s), 1572 (m), 1476 (vs), 1451 (s), 1287 (vs), 1270 (vs), 1107 (m), 1015 (m), 889 (s), 782 (m), 749 (s), 610 (m), 602 (m), 540 (m), 512 (m), 427 cm⁻¹ (m); ¹H NMR ([D₆]benzene, RT, 200 MHz): δ = 1.06 (m, 2H; COD), 1.38 (m, 2H; COD), 1.50 (m, 2H; COD), 2.11 (s, 15H; Cp*), 2.12 (m, 2H; COD), 3.49 (m, 4H; COD), 3.51 (d, J = 12.82 Hz, 2H; OCH₂), 4.68 (d, J = 12.82 Hz, 2H; OCH₂), 6.67 (m, 2H; Ar), 6.79 (m, 2H; Ar), 6.95 (m, 2H; Ar), 7.08 ppm (m, 2H; Ar); ¹³C{¹H} NMR: δ = 12.1 (s, Cp*), 29.7 (s, COD), 30.7 (s, COD), 69.0 (s, OCH₂), 73.8 (d, J = 14.9 Hz, COD), 74.5 (d, J = 14.9 Hz, COD), 117.2 (s, Ar), 117.9 (s, Ar), 125.6 (s, Ar), 126.2 (s, Cp*), 129.5 (s, Ar), 165.0 ppm (s, *ipso*); elemental analysis calcd (%) for C₃₂H₃₉O₄RhTi: C 60.20, H 6.15; found: C 60.06, H 6.45.

[TiCp*(O₂Bz)₂Ir(cod)] (4): Toluene (3 mL) was added to a mixture of **1** (0.067, 0.16 mmol) and [[Ir(μ -OH)(cod)]₂] (0.050, 0.16 mmol) at room temperature. The mixture was stirred for 1 h, the solvent was removed under vacuum and the residue washed with pentane to yield **4** as a yellow solid. Yield: 0.060 g, 53%; IR: $\tilde{\nu}$ = 1595 (s), 1572 (m), 1476 (vs), 1452 (s), 1285 (vs), 1267 (vs), 1110 (w), 1007 (m), 891 (m), 882 (m), 751 (s), 630 (m), 553 (m), 512 (m), 430 cm⁻¹ (m); ¹H NMR ([D₆]benzene, RT, 200 MHz): δ = 0.97 (m, 2H; COD), 1.32 (m, 2H; COD), 1.49 (m, 2H; COD), 2.06 (s, 15H; Cp*), 2.10 (m, 2H; COD), 3.52 (m, 2H; COD), 3.63 (m, 2H; COD), 4.02 (d, J = 12.82 Hz, 2H; OCH₂), 4.84 (d, J = 12.82 Hz, 2H; OCH₂), 6.64 (m, 2H; Ar), 6.79 (m, 2H; Ar), 6.90 (m, 2H; Ar), 7.03 ppm (m, 2H; Ar); ¹³C{¹H} NMR: 12.1 (s, Cp*), 30.7 (s, COD), 31.9 (s, COD), 55.4 (s, COD), 56.1 (s, COD), 69.8 (s, OCH₂), 117.2 (s, Ar), 118.5 (s, Ar), 125.7 (s, Cp*), 125.9 (s, Ar), 129.6 (s, Ar), 164.6 ppm (s, *ipso*); elemental analysis calcd (%) for C₃₂H₃₉O₄IrTi: C 52.81, H 5.40; found: C 52.86, H 5.29.

[TiCp*(O₂Bz)₂Rh(CO)] (5): A suspension of **3** (0.108 g, 0.17 mmol) in hexane was treated with an excess of CO at room temperature, and the resulting solution was cooled to -30 °C to yield orange crystals of **5**. Yield: 0.073 g, 73%; IR: $\tilde{\nu}$ = 2066 (vs), 1997 (vs), 1595 (m), 1573 (w), 1476 (s), 1454 (s), 1278 (s), 1254 (s), 1110 (w), 990 (m), 880 (m), 782 (w), 754 (s), 630 (w), 613 (m), 530 (w), 512 (m), 427 cm⁻¹ (m); ¹H NMR ([D₆]benzene, RT, 200 MHz): δ = 1.96 (s, 15H; Cp*), 4.16 (d, J = 12.46 Hz, 2H; OCH₂), 4.90 (dd, J = 12.46, 2.56 Hz, 2H; OCH₂), 6.66 (m, 2H; Ar), 6.86 (m, 4H; Ar), 7.06 ppm (m, 2H; Ar); ¹³C{¹H} NMR: 12.3 (s, Cp*), 76.6 (s, OCH₂), 116.9 (s, Ar), 118.7 (s, Ar), 126.3 (s, Ar), 126.8 (s, Cp*), 130.3 (s, Ar), 164.1 (s, *ipso*), 183.4 (d, J = 73 Hz, CO), 196.6 ppm (s, *ipso*); elemental analysis calcd (%) for C₂₆H₂₇O₆RhTi: C 53.20, H 4.64; found: C 53.58, H 4.89.

[TiCp*(Me)((OCH₂)₂Py)] (2): 2,6-Pyridinedimethanol (0.326 g, 2.34 mmol) was added to a solution of [TiCp*(Me)₃] (0.535 g, 2.34 mmol) in toluene (8 mL) at room temperature. The mixture was stirred for 4 h, and after filtration the solvent was removed under vacuum and the residue washed with pentane to yield bright yellow **2**. Yield: 0.647 g, 78%; IR: $\tilde{\nu}$ = 1607 (m), 1575 (m), 1476 (m), 1451 (m), 1317 (m), 1098 (vs), 1064 (s), 795 (m), 759 (vs), 737 (m), 613 (m), 486 (s), 480 (cm⁻¹) (s); ¹H NMR ([D₆]benzene, RT, 200 MHz): δ = 0.12 (s, 3H; TiMe), 2.11 (s, 15H; Cp*), 5.49 (d, J = 16.5 Hz, 2H; CH₂), 5.60 (d, J = 16.5 Hz, 2H; CH₂), 6.30 (m, 2H; Ar), 6.73 ppm (m, 1H; Ar); ¹³C{¹H} NMR: 11.7 (s, Cp*), 41.8 (s, TiMe), 78.9 (s, CH₂), 115.4 (s, Ar), 120.9 (s, Cp*), 137.5 (s, Ar), 168.3 ppm (s, *ipso*); elemental analysis calcd (%) for C₁₅H₂₅O₂NiTi: C 64.48, H 7.51, N 4.17; found: C 63.95, H 7.21, N 4.01.

[TiCp*((OCH₂)₂Py)(μ -O)Rh(cod)] (6): Toluene (4 mL) was added to a mixture of **2** (0.075 g, 0.22 mmol) and [[Rh(μ -OH)(cod)]₂] (0.051 g, 0.22 mmol) at room temperature. The mixture was stirred for 10 min and then the solvent was partially evaporated under vacuum. Slow diffusion of pentane into the toluene solution yielded yellow crystals of **6**. Yield: 0.064 g, 52%; IR: $\tilde{\nu}$ = 1595 (m), 1578 (m), 1464 (m), 1435 (m), 1336 (m), 1098 (vs), 1074 (s), 795 (s), 759 (vs), 737 (m), 487 (m), 475 cm⁻¹ (m); ¹H NMR ([D₆]benzene, RT, 200 MHz): δ = 1.34 (m, 4H; COD), 1.95 (m, 4H; COD), 2.13 (s, 15H; Cp*), 3.32 (m, 1H; COD), 3.83 (m, 1H; COD), 3.98 (m, 2H; COD), 4.42 (d, J = 16.86 Hz, 1H; OCH₂), 4.88 (d, J = 16.86 Hz, 1H; OCH₂), 5.29 (d, J = 18.33 Hz, 1H; OCH₂), 5.54 (d, J = 18.33 Hz, 1H; OCH₂), 6.10 (m, 2H; Ar), 6.66 ppm (m, 1H; Ar); elemental analysis calcd (%) for C₂₅H₃₄O₃NrRhTi: C 54.87, H 6.26, N 2.56; found: C 54.88, H 6.47, N 2.48.

[TiCp*((OCH₂)₂Py)(μ -O)Ir(cod)] (7): Toluene (3 mL) was added to a mixture of **2** (0.089 g, 0.26 mmol) and [[Ir(μ -OH)(cod)]₂] (0.085 g, 0.26 mmol) at room temperature. The mixture was stirred for 2 h, the solvent evaporated under vacuum and the residue washed with pentane to yield yellow **7**. Yield: 0.076 g, 45%; IR: $\tilde{\nu}$ = 1597 (m), 1578 (m), 1466 (m), 1435 (m), 1335 (m), 1098 (s), 1072 (s), 796 (m), 756 (m), 736 (vs), 485 cm⁻¹ (s); ¹H NMR ([D₆]benzene, RT, 200 MHz): δ = 1.19 (m, 4H; COD), 1.94 (m, 4H; COD), 2.05 (s, 15H; Cp*), 3.27 (m, 1H; COD), 3.92 (m, 2H; COD), 4.08 (m, 1H; COD), 4.60 (d, J = 16.86 Hz, 1H; OCH₂), 4.95 (d, J = 16.86 Hz, 1H; OCH₂), 5.18 (d, J = 19.06 Hz, 1H; OCH₂), 5.48 (d, J = 19.06 Hz, 1H; OCH₂), 6.06 (m, 2H; Ar), 6.64 ppm (m, 1H; Ar); ¹H NMR (CDCl₃, RT, 200 MHz): δ = 1.57 (m, 4H; COD), 2.25 (m, 4H; COD), 2.01 (s, 15H; Cp*), 3.39 (m, 1H; COD), 3.59 (m, 1H; COD), 3.76 (m, 1H; COD), 3.99 (m, 1H; COD), 4.74 (d, J = 17.23 Hz, 1H; OCH₂), 5.32 (d, J = 18.33 Hz, 1H; OCH₂), 5.41 (d, J = 17.23 Hz, 1H; OCH₂), 5.65 (d, J = 18.33 Hz, 1H; OCH₂), 7.05 (m, 2H; Ar), 7.69 ppm (m, 1H; Ar); ¹³C{¹H}

Table 3. Crystal data for **3**, **5** and **7**.

	3	5	7
formula	C ₃₂ H ₃₉ O ₄ RhTi	C ₂₆ H ₂₇ O ₆ RhTi	C ₂₅ H ₃₄ IrNO ₃ Ti
M_r	638.44	586.29	636.63
T [K]	293(2)	293(2)	293(2)
crystal system	orthorhombic	monoclinic	monoclinic
space group	<i>Pbca</i>	<i>C2/c</i>	<i>P2₁/n</i>
a [Å]	17.146(2)	27.162(3)	14.765(1)
b [Å]	14.721(5)	12.134(1)	15.007(2)
c [Å]	22.727(4)	17.412(5)	21.892(4)
β [°]		91.51(2)	91.64(1)
V [Å ³]	5736(2)	5737(2)	4849(1)
Z	8	8	8
ρ [g cm ⁻³]	1.478	1.358	1.744
μ [cm ⁻¹]	8.89	8.87	58.38
$F(000)$	2640	2384	2512
index ranges	0 ≤ h ≤ 22 0 ≤ k ≤ 19 -29 ≤ l ≤ 40	-35 ≤ h ≤ 0 -15 ≤ k ≤ 0 -22 ≤ l ≤ 22	-16 ≤ h ≤ 16 0 ≤ k ≤ 16 0 ≤ l ≤ 24
reflection collected	7642	6870	7338
independent reflection	6807 [$R(\text{int}) = 0.0316$]	6737 [$R(\text{int}) = 0.0206$]	7128 [$R(\text{int}) = 0.1451$]
data/restraints/parameters	6807/0/348	6737/0/312	7128/0/309
GOF on F^2	0.877	0.980	0.968
R_1/wR_2 [$I > 2\sigma(I)$]	0.0653/0.0905	0.0534/0.1194	0.1072/0.2464
max/min residual electron density [e Å ⁻³]	0.474/ -1.153	0.788/ -0.462	1.683/ -1.249

NMR (CDCl₃, RT): 12.0 (s, Cp*), 30.2 (s, COD), 30.4 (s, COD), 31.4 (s, COD), 32.5 (s, COD), 73.2 (s, COD), 73.4 (s, COD), 74.6 (s, CH₂), 75.8 (s, COD), 76.0 (s, CH₂), 76.2 (s, COD), 116.0 (s, Ar), 117.0 (s, Ar), 119.5 (s, Ar), 139.2 (s, Cp*), 163.1 (s, *ipso*), 169.7 ppm (s, *ipso*); elemental analysis calcd (%) for C₂₅H₃₄O₃NiRfTi: C 47.17, H 5.38, N 2.20; found: C 47.35, H 5.42, N 2.13.

X-ray crystallography: Suitable crystals of **3**, **5** and **7** were mounted in glass capillaries and sealed under nitrogen. Crystallographic data are listed in Table 3.

Data were collected on a Nonius-Mach3 diffractometer with MoK α radiation (graphite monochromator, $\lambda = 0.71073$ Å) with a ω - 2θ scan technique to a maximum value of 56 °C. The intensities were corrected for Lorentzian and polarisation effects, and for **7** empirical absorption correction was carried out on the basis of an azimuthal scan.^[26] The structures were solved by direct method with the SHELXS97^[27] program. Refinement on F^2 was carried out by full-matrix least-squares techniques with the SHELXL97 program. For **3** and **5**, all non-hydrogen atoms were refined with anisotropic thermal parameters. The hydrogen atoms were included in calculated positions and were refined isotropically. The crystal of **7** was of poor quality and diffracted rather weakly. Attempts were made to refine all the atoms anisotropically, but led to negative anisotropic displacement parameters. Therefore only the Ir, Ti and O atoms were refined isotropically.

CCDC 185718 (**3**), 185719 (**5**) and 185720 (**7**) contain the supplementary crystallographic data for this paper. These data can be obtained free of charge via www.ccdc.cam.ac.uk/conts/retrieving.html (or from the Cambridge Crystallographic Data Centre, 12 Union Road, Cambridge CB2 1EZ, UK; fax: (+44) 1223-336-033; or deposit@ccdc.cam.ac.uk).

Acknowledgements

This work was supported by the Dirección General de Enseñanza Superior e Investigación Científica (Spain, Grant No. PB 98–0159-C02–01) and Ministerio de Ciencia y Tecnología, Spain (MAT2001–2215-C03–01). We thank Dr. M. A. Peña for recording the XPS spectra.

- [1] a) A. W. Holland, D. S. Gluck, R. G. Bergman, *Organometallics* **2001**, *20*, 2250; b) K. N. Raymond, C. J. Carrano, *Acc. Chem. Res.* **1979**, *12*, 183; c) M. Elhabiri, P. Figueirido, K. Toki, N. Saito, R. Brouillard, *J. Chem. Soc. Perkin Trans.* **1997**, 355; d) K. Gigant, A. Rammal, M. Henry, *J. Am. Chem. Soc.* **2001**, *123*, 11632.
- [2] J. Okuda, S. Fokken, T. Kleinhenn, T. P. Spaniol, *Eur. J. Inorg. Chem.* **2000**, 1321.
- [3] a) S. J. Sturla, S. L. Buchwald, *Organometallics* **2002**, *21*, 739 and references therein; b) N. W. Eilerts, J. A. Heppert, M. L. Kennedy, F. Takusagawa, *Inorg. Chem.* **1994**, *33*, 4813.
- [4] R. T. Toth, D. W. Stephan, *Can. J. Chem.* **1991**, *69*, 172.
- [5] a) R. Fandos, C. Hernández, A. Otero, A. Rodríguez, M. J. Ruiz, P. Terreros, *Organometallics* **1999**, *18*, 2718; b) R. Fandos, J. L. Fierro, M. M. Kubicki, A. Otero, P. Terreros, M. A. Vivar-Cerrato, *Organometallics* **1995**, *14*, 2162; c) D. Selent, P. Claus, J. Pckardt, *J. Organomet. Chem.* **1994**, *468*, 131; d) M. S. Rau, C. M. Kretz, G. L. Geoffroy, A. L. Rheingold, B. S. Haggerty, *Organometallics* **1994**, *13*, 1624 and references therein; e) R. Xi, B. Wang, M. Abe, Y. Ozawa, K. Isobe, *Chem. Lett.* **1994**, 1177; f) R. Xi, B. Wang, M. Abe, Y. Ozawa, K. Isobe, *Chem. Lett.* **1994**, 323; g) K. Isobe, A. Yagasaki, *Acc. Chem. Res.* **1993**, *26*, 524.
- [6] S. J. Tauster, *Acc. Chem. Res.* **1987**, *20*, 389.
- [7] a) A. O. Bouth, G. L. Rice, S. L. Scott, *J. Am. Chem. Soc.* **1999**, *121*, 7201; b) P. Dufour, S. L. Scott, C. C. Santini, F. Lefebvre, J.-M. Basset, *Inorg. Chem.* **1994**, *33*, 2509.
- [8] A. I. Gouzyr, H. Wessel, C. E. Barnes, H. W. Roesky, M. Teichert, I. Usón, *Inorg. Chem.* **1997**, *36*, 3392.
- [9] a) C. D. Chandler, J. Caruso, M. J. Hampden-Smith, A. L. Rheingold, *Polyhedron* **1995**, *14*, 2491; b) B. A. Vaartstra, J. C. Huffman, P. S. Gradoff, L. G. Hubert-Pfalzgraf, J. C. Daran, S. Parraud, K. Yunlin, K. G. Caulton, *Inorg. Chem.* **1990**, *29*, 3126.
- [10] K. Nomura, N. Naga, M. Miki, K. Yanagi, A. Imai, *Organometallics* **1998**, *17*, 2152.
- [11] A. V. Firth, D. W. Stephan, *Inorg. Chem.* **1998**, *37*, 4732.
- [12] V. W. Day, T. A. Eberspacher, J. Hao, W. G. Klemperer, B. Zhong, *Inorg. Chem.* **1995**, *43*, 3549.
- [13] S. Sakellson, M. McMillan, G. L. Haller, *J. Phys. Chem.* **1986**, *90*, 1733.
- [14] a) S. Rojas, J. L. García-Fierro, R. Fandos, A. Rodríguez, P. Terreros, *J. Chem. Soc. Dalton Trans.* **2001**, 2316; b) M. A. Ciriano, F. Viguri, J. J. Pérez-Torrente, F. J. Lahoz, L. A. Oro, A. Tiripicchio, M. Tiripicchio-Camellini, *J. Chem. Soc. Dalton Trans.* **1989**, 25.
- [15] A. C. Yang, C. W. Garland, *J. Chem. Soc.* **1957**, *61*, 1504.
- [16] a) F. Bottomley, I. J. B. Lin, P. S. White, *J. Am. Chem. Soc.* **1981**, *103*, 704; b) J. Okuda, E. Herdtweck, *Inorg. Chem.* **1991**, *30*, 1516; c) T. J. Clark, T. A. Nile, D. McPhail, A. T. McPhail, *Polyhedron*, **1989**, *8*, 1804; d) P. Gómez-Sal, A. M. Irigoyen, M. Mena, M. Monge, C. Yélamos, *J. Organomet. Chem.* **1995**, *494*, C19.
- [17] M. A. Casado, M. A. Ciriano, A. J. Edwards, F. J. Lahoz, L. A. Oro, J. J. Pérez-Torrente, *Organometallics* **1999**, *18*, 3025.
- [18] a) G. Bond S. Flamerz, *Appl. Catal.* **1989**, *46*, 89; b) C. U. I. Odenbrand, S. L. T. Andersson, L. A. H. Andersson, J. G. M. Brandin, G. Busca, *J. Catal.* **1990**, *125*, 541.
- [19] a) S. Hamoudi, F. Larachi, A. Sayari, *Catal. Lett.* **2001**, *77*, 227; b) M. C. Capel-Sanchez, J. M. Campos-Martin, J. L. G. Fierro, M. P. De Frutos, A. Padilla Polo, *Chem. Commun.* **2000**, 855.
- [20] R. Fandos, A. Otero, A. Rodríguez, M. J. Ruiz, P. Terreros, *Angew. Chem.* **2001**, *113*, 2968; *Angew. Chem. Int. Ed.* **2001**, *40*, 2884.
- [21] a) C. Furlani, G. Mattogno, G. Polzonetti, *Inorg. Chim. Acta.* **1983**, *69*, 199; b) C. Furlani, G. Mattogno, G. Polzonetti, G. Sbrana, G. Valentini, *J. Catal.* **1985**, *94*, 335; c) P. Terreros, E. Pastor, J. M. Palacios, J. L. G. Fierro, *Surf. Interface Anal.* **1990**, *15*, 279.
- [22] a) J. Evans, B. E. Hayden, F. Mosselmans, A. Murray, *Surf. Sci.* **1994**, *301*, 61; b) J. Evans, B. E. Hayden, M. A. Newton, *Surf. Sci.* **2000**, *462*, 169.
- [23] M. Mena, M. A. Pellinghelli, P. Royo, R. Serrano, A. Tiripicchio, *J. Chem. Soc. Chem. Commun.* **1986**, 1118.
- [24] a) R. Usón, L. A. Oro, J. A. Cabeza, *Inorg. Synth.* **1985**, *23*, 126; b) D. Selent, M. Ramm, *J. Organomet. Chem.* **1995**, *485*, 135.
- [25] L. M. Green, D. W. Meek, *Organometallics* **1989**, *8*, 659.
- [26] A. C. T. North, D. C. Phillips, F. S. Mathews, *Acta Crystallogr. Sect. A* **1968**, *24*, 351.
- [27] SHELXS-97, Programs for crystal structure analysis (Release 97–2). G. M. Sheldrick, Universität Göttingen, Göttingen, Germany, **1997**.

Received: May 21, 2002
Revised: October 8, 2002 [F4111]